

Supporting Information for:

**Inducible Biosynthetic Nanoscaffolds as Recruitment Platforms for Detecting
Molecular Target Interactions Inside Living Cells**

Sangkyu Lee,^{†,§} Jae-Seok Ha,^{¶,§} Seung-Goo Lee,[‡] and Tae K. Kim^{¶,*}

*Korea Advanced Institute of Science and Technology,[†] Daejeon, Korea,
Korea Research Institute of Bioscience and Biotechnology,[‡] Daejeon, Korea,
Reons Innovative Medicines Institute,[¶] Anyang, Gyeonggi-do, Korea,
Unist-Olympus Biomed Imaging Center, School of Nano-Biotechnology and Chemical
Engineering, Ulsan National Institute of Science and Technology,^{*} Ulsan, Korea.*

E-mail: tkkim@reonsimi.com

Methods

DNA constructions

cDNA encoding human ferritin light subunit (FT; GeneBank Acc. No. BC016346) was cloned into *KpnI* and *BamHI* sites of pcDNA3.1 (Invitrogen), and then mCerulean PCR product was cloned into *AflIII* and *KpnI* sites of that plasmid, resulting in mCerulean-FT. Subsequently, cDNAs of FRB and FKBP were fused by overlap extension PCR with *NheI* and *AflIII* sites at the 5' and 3' ends of the genes, respectively. The restricted product was then cloned in-frame into *NheI* and *AflIII* sites of mCerulean-FT for generating FRB-FKBP-mCerulean-FT plasmid. Coding region of mCerulean from mCerulean-FT was excised by *NheI* and *KpnI* and replaced with haloalkane dehalogenase and O⁶-alkylguanine-DNA alkyltransferase for HD-FT and AGT-FT plasmids, respectively. For generating Zip1-FT or Zip2-EGFP plasmids, Zip1 (ALK KEL QANK KEL AQL KWEL QAL KKE LAQ) or Zip2 (EQLE KKL QALE KKL AQL EWKN QAL EKK LAQ)¹ was fused to N-terminus of human ferritin heavy subunit (GeneBank Acc. No. BC016009) or EGFP, respectively. FYVE domain (274-349) of FENS1 was excised by *BglII* and *KpnI* and fused to the C-terminus of EYFP (EYFP-C1, Clontech) to generate EYFP-FYVE_{FENS1} plasmid. Constructions of plasmids for FRB-EGFP-FT, FRB-mRFP-FT, FKBP-mRFP-FT, IκBα-ECFP-FT, EYFP-RelA, and DHFR-mRFP-FT were described previously.² Plasmid of FRB-mCherry-Rab5B was described in elsewhere.³

Cell culture and transfection

HeLa cells were maintained in DMEM (Invitrogen) supplemented with 10 % fetal bovine serum (FBS, Invitrogen) at 37°C and 5% CO₂. Transfection was performed using a MicroporatorTM (MP-100; Digital Bio Technology) and Lipofectamine[®]2000 (Invitrogen) according to the manufacturer's instructions. The optimized conditions of electroporation for HeLa cell were 2 pulses of 1080V for 35 millise.

Molecular target interaction assay

At 24 h after transfection, medium was replaced with OPTI-MEM (Invitrogen) and treated with selected concentrations of rapamycin (Calbiochem). For competition experiments, transfected cells were pre-incubated with 25 μM FK506 (Sigma) for 10 min before treatment with rapamycin. For analyzing interactions of human and *E.coli* DHFR with their small molecule ligands (DHFR Ligand-FL and *E.coli* DHFR Ligand-FL), transfected cells were incubated with 10 μM methotrexate-FL (Invitrogen) and

trimethoprim-FL (Active Motif) ligands according to the manufacture's protocols and then treated with 500 nM rapamycin. For analyzing interactions of HD (haloalkane dehalogenase) and AGT (O⁶-alkylguanine-DNA alkyltransferase) with their small molecule ligands (HD Ligand-FL, HD Ligand-TMR, and AGT Ligand-FL), transfected cells were incubated with HaloTag-Oregon Green (Promega), HaloTag-TMR (Promega), and SNAP-Cell 505 (NEB) ligands according to the manufacture's protocols and then treated with 500 nM rapamycin. For quantitative analysis, cells were fixed with 4 % formaldehyde and washed with DPBS.

Confocal imaging

Confocal microscopy was performed on the Nikon A1R with a CFI Plan Apochromat VC objective lens (60x/1.40NA) along with digital zooming of NIS-element software (Nikon) according to the manufacturer's instructions. For acceptor bleaching FRET, 10 pulses of laser were stimulated without delay and fluorescent images for donor and acceptor were captured simultaneously.

Image processing and analysis

Confocal images were stored as a ND2 (or JPEG2000) file format. Cropping of images was performed with MetaMorph offline version 7.6.0.0 (MDS Analytical Technologies). ND2 files were converted into ICS format and the "Make Movie" tool in the MetaMorph software was used to make video files. For quantification of nanocluster formation, nanoclusters were defined as discrete punctated dots of fluorescence with criteria of fluorescent intensity (2500-4095), size ($>0.2 \text{ m}^2$), and circularity (0.5-1.0). Number and size of nanoclusters per cells were measured with the "Object Count" tool in Nikon imaging software (NIS-element AR 64-bit version 3.10, Laboratory Imaging). Co-localization between two molecules with different fluorescent colors was measured by using "Co-localization" tool in Nikon imaging software. To visualize changes of fluorescent intensities and patterns in the course of nanocluster formation, the "Intensity Surface Plot" tool in the NIS-element software was used. Donor and acceptor intensities in FRET analysis were measured by using the "Time Measurement" tool in Nikon imaging software.

Supplementary Videos

Video S1. Specific nanocluster formation induced by FKBP-rapamycin-FRB interactions inside living cells. HeLa cells transfected with FRB-FKBP-mCerulean-FT were treated with 500 nM rapamycin to trigger FKBP-FRB heterodimerization and induce nanocluster formation. Images for FRB-FKBP-mCerulean-FT were captured in every 20 sec for 20 min. Rapamycin was added at 1 min after imaging.

Video S2. Specific nanocluster formation induced by FKBP-rapamycin-FRB interactions inside living cells. HeLa cells co-transfected with FRB-EGFP-FT and FKBP-mRFP-FT were treated with 500 nM rapamycin. Images were captured in every 10 sec for 5 min. Rapamycin was added at 1 min after imaging.

Video S3. Visualizing specific interactions of DHFR with its small molecule ligand on inducibly assembled nanoclusters/nanoscaffolds. HeLa cells co-transfected with FRB-FKBP-mCerulean-FT and DHFR-mRFP-FT were incubated with 10 μ M DHFR Ligand-FL prior to treatment with 500 nM rapamycin. Images were captured in every 1 min for 10 min. Rapamycin was added at 1 min after imaging.

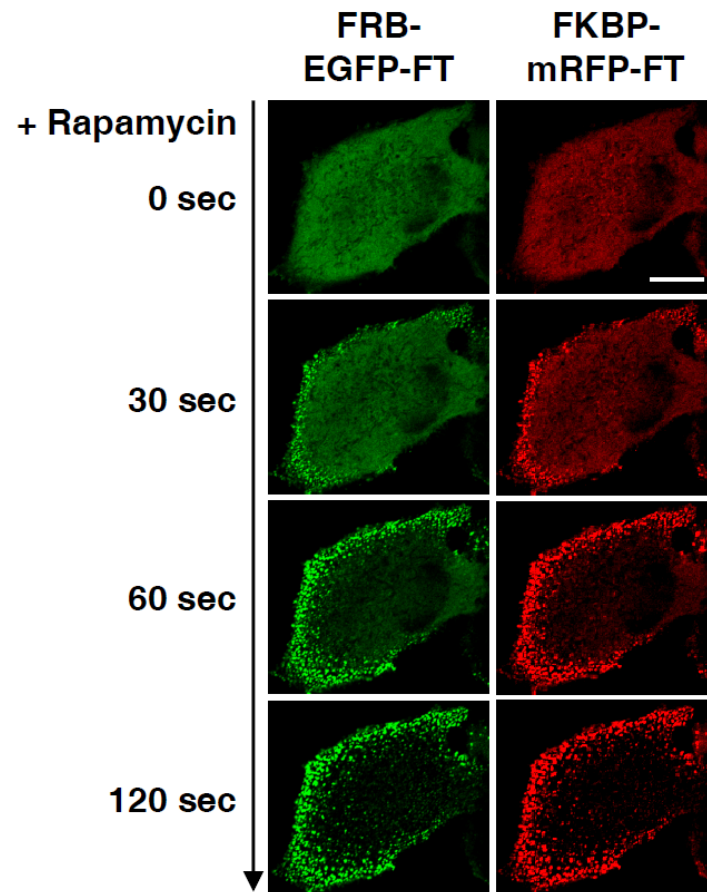


Figure S1. Time-lapse images for visualizing nanocluster formation by interactions of rapamycin with FKBP and FRB inside living cells. HeLa cells were co-transfected with expression plasmids as indicated and then treated with 500 nM rapamycin. Scale bar = 20 μm.

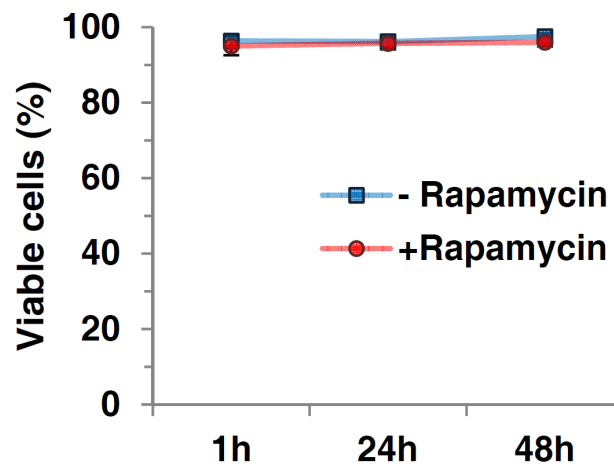


Figure S2. Effect of nanocluster formation on cell viability. HeLa cells transfected with FRB-FKBP-mCerulean-FT were treated with 500 nM rapamycin for three different incubation periods (1, 24, and 48h). Incubated cells were harvested and stained with trypan blue to measure the percentages of viable cells. For each time point, over 300 cells were counted to measure the average value of cell viability. Error bars, s.d.

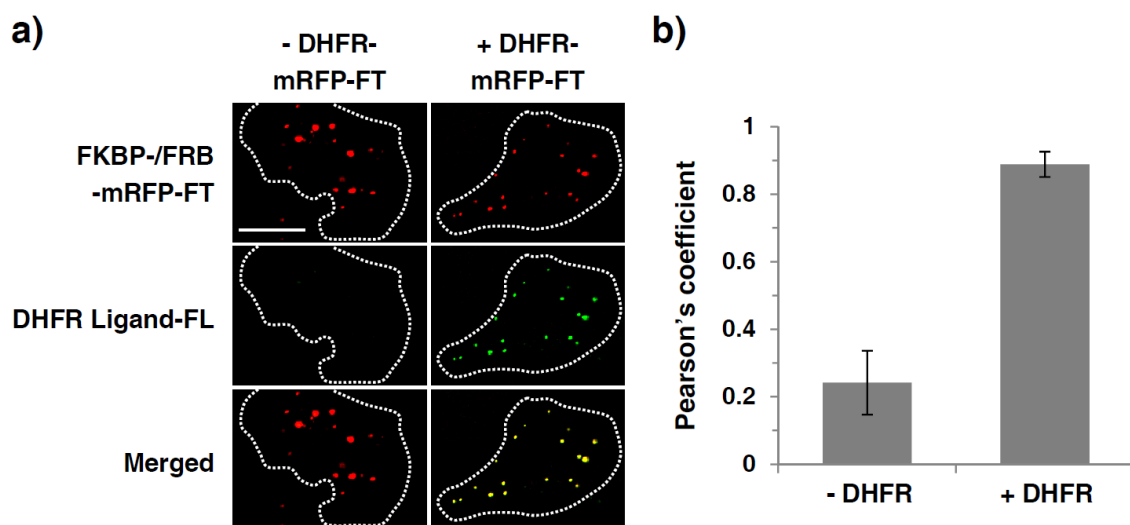


Figure S3. Visualization of specific interactions of DHFR with its small molecule ligand on assembled biosynthetic nanoscaffolds. (a) HeLa cells co-transfected with expression plasmids as indicated were incubated with 10 μ M DHFR Ligand-FL (fluorescein-labeled methotrexate) prior to treatment with 500 nM rapamycin. Dashed line indicates cell boundary. (b) Co-localization of DHFR with DHFR Ligand-FL was analyzed by measuring Pearson's correlation coefficient. Scale bar = 20 μ m.

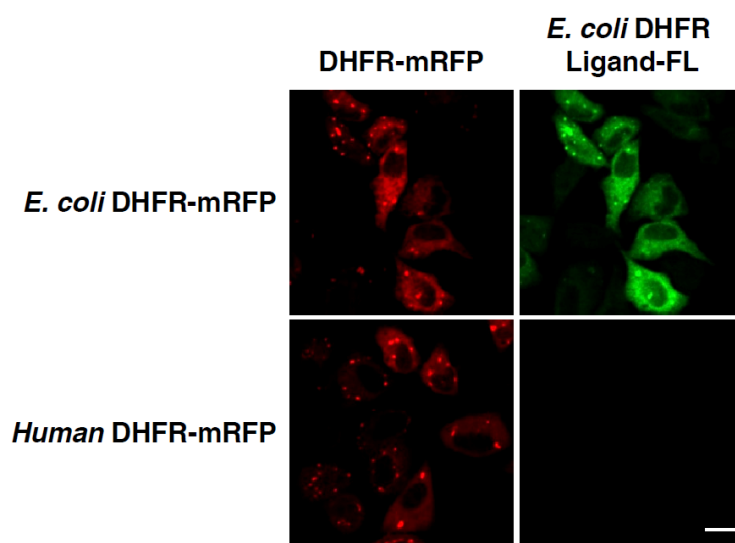


Figure S4. Visualization of species-specific interactions of DHFR with its small molecule ligand on assembled biosynthetic nanoscaffolds. HeLa cells expressing *E.coli* or human DHFR-mRFP displayed on FT-derived nanoclusters were incubated with 100 nM *E.coli* DHFR Ligand-FL (fluorescein-labeled trimethoprim). Scale bar = 20 μ m.

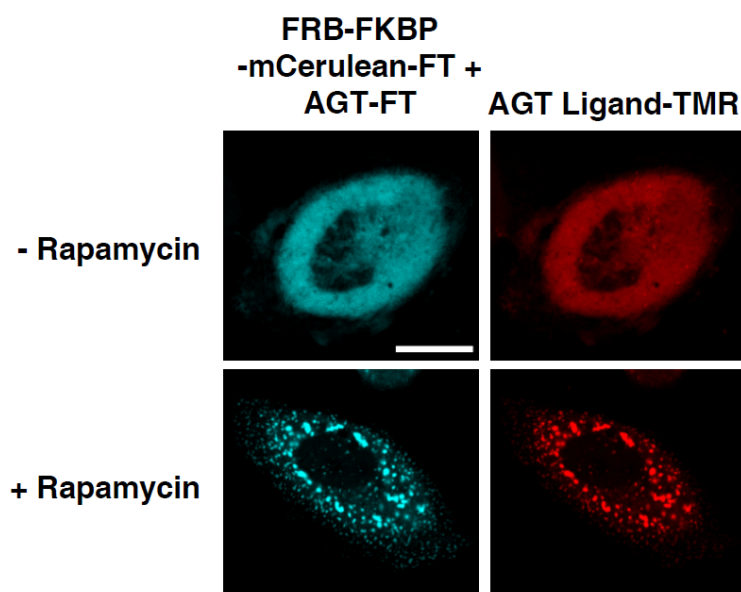


Figure S5. Visualization of specific interactions of AGT with its small molecule ligand on assembled biosynthetic nanoscaffolds. HeLa cells co-transfected with expression plasmids as indicated were incubated with 5 μ M AGT Ligand-TMR prior to treatment with 500 nM rapamycin. Scale bar = 20 μ m.

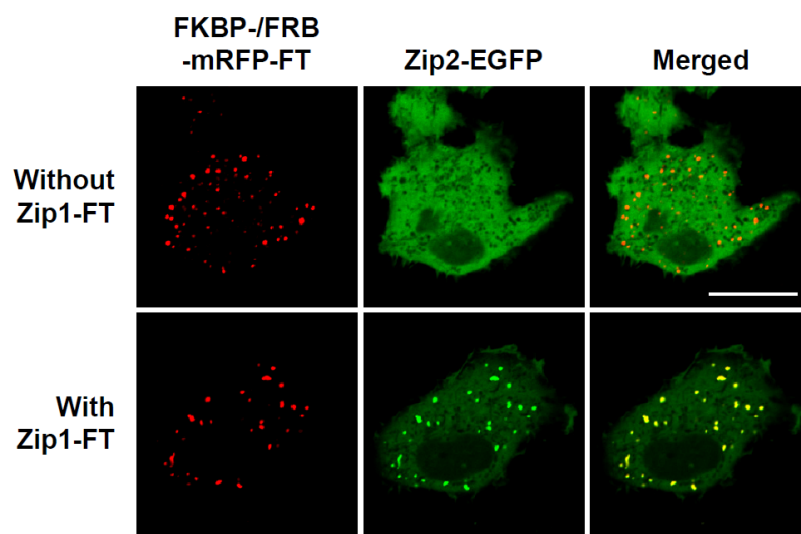


Figure S6. Detection of leucine zipper interactions on assembled biosynthetic nanoscaffolds. HeLa cells co-transfected with expression plasmids as indicated were treated with 500 nM rapamycin. Scale bar = 20 μ m.

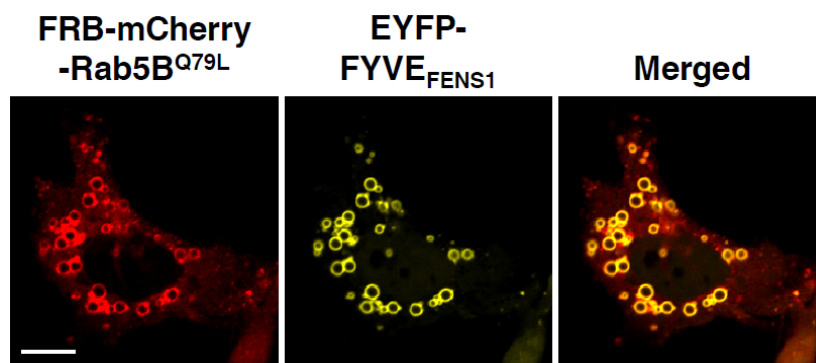


Figure S7. Co-localization of Rab5B with FYVE domain of FENS1 in endosomes. Fluorescent images of HeLa cells co-expressing endosomal localized proteins of FRB-mCherry-Rab5B^{Q79L} and EYFP-labeled FYVE domain were captured. Scale bar = 20 μm .

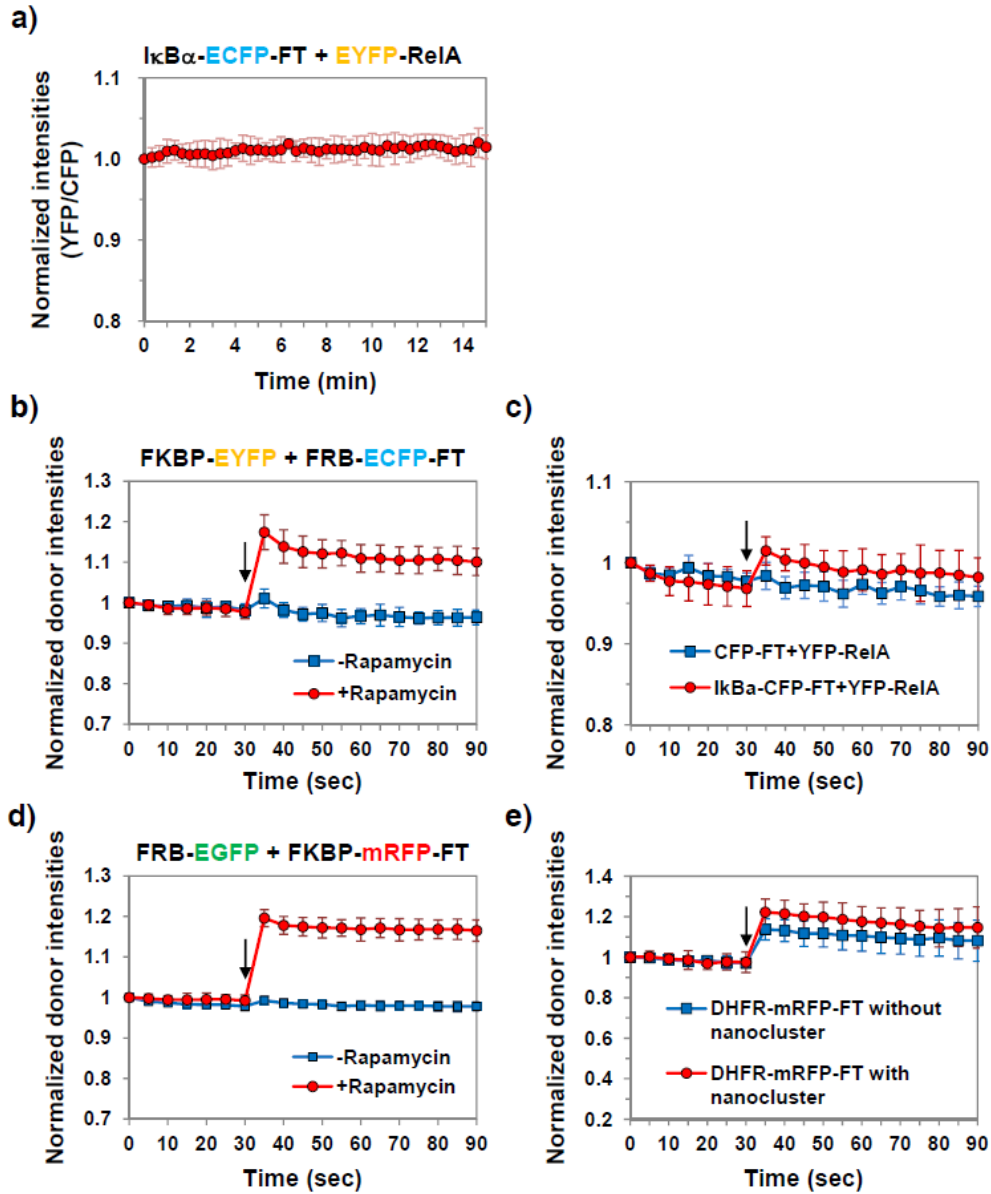


Figure S8. Analysis of IκBα-RelA and DHFR-methotrexate interactions with FRET. (a) Normalized ratio of YFP to CFP intensities in live HeLa cells co-expressing EYFP-RelA and IκBα-ECFP-FT. Images were captured in every 20 sec for 15 min. (b-e) Acceptor bleaching FRET analyzed in fixed HeLa cells co-transfected with expression plasmids as indicated. Intensities of donor (CFP or GFP) were quantified and normalized before and after bleaching of acceptor (YFP or RFP). For analyzing DHFR-methotrexate interaction, HeLa cells were incubated with 10 μM fluorescein-labeled methotrexate with or without nanocluster formation. Arrow indicates the timepoint for acceptor bleaching. Images were captured in every 5 sec.

Table S1. Comparison of nanocluster assay with previously developed technologies for molecular target interactions

Method	Pros	Cons	Ref
Affinity purification	<ul style="list-style-type: none"> - Easy manipulation of binding conditions - Detection of endogenous target protein(s) with specific antibody 	<ul style="list-style-type: none"> - <i>In vitro</i> binding conditions - High false positives/negatives - Hard to detect dynamic interactions - Laborious procedure - Ensemble averaging over heterogenous cell populations 	5-10
Yeast three hybrid	<ul style="list-style-type: none"> - Easy to genetic manipulation - Suitable for screening 	<ul style="list-style-type: none"> - Indirect readout - Non-mammalian cells - High false positives/negatives - Hard to detect dynamic interactions - Required to translocate into the nucleus of bait and prey - Not applicable to single cell level 	4-7,11,12
BiFC	<ul style="list-style-type: none"> - Direct readout - Rapid analysis - Applicable to live cell - Single cell analysis - Suitable for screening - Applicable to subcellular organelles 	<ul style="list-style-type: none"> - Delayed readout - Careful consideration of fusion protein constructions - Hard to quantify binding kinetics 	13-15
FRET	<ul style="list-style-type: none"> - Direct readout - Rapid analysis - Applicable to live cell - Single cell analysis - Applicable to subcellular organelles - Monitoring molecular dynamics and kinetics 	<ul style="list-style-type: none"> - Relatively low sensitivity - Not suitable for screening diverse molecular interactions at the same time - Careful consideration of fluorescence pair and fusion protein constructions 	13,16-19

Recruitment/ redistribution	<ul style="list-style-type: none"> - Direct readout - Rapid analysis - Applicable to live cell - Single cell analysis - Suitable for screening 	<ul style="list-style-type: none"> - Background signals caused by molecules inherently localized at the recruitment sites - Hard to quantify binding kinetics - Hard to apply to interactions within intracellular small organelles 	13,20-23
Nanocluster-based recruitment/ redistribution	<ul style="list-style-type: none"> - Direct readout - Rapid analysis - Applicable to live cell - Single cell analysis - Suitable for screening - High sensitivity and selectivity - Synthetic recruitment site independent of intracellular compartments 	<ul style="list-style-type: none"> - Hard to quantify binding kinetics - Hard to apply to interactions within intracellular small organelles 	2

References

1. Magliery, T. J.; Wilson, C. G.; Pan, W.; Mishler, D.; Ghosh, I.; Hamilton, A. D.; Regan, L. *J Am Chem Soc* **2005**, *127*, 146-157.
2. Lee, S.; Lee, K. H.; Ha, J. S.; Lee, S. G.; Kim, T. K. *Angew. Chem. Int Ed* **2011**, *50*, 8709-8713.
3. Lee, K. H.; Lee, S.; Lee, W. Y.; Yang, H. W.; Heo, W. D. *Proc Natl Acad Sci U S A* **2010**, *107*, 3412-3417.
4. Stockwell, B. R. *Nature* **2004**, *432*, 846-854.
5. Burdine, L.; Kodadek, T. *Chem Biol* **2004**, *11*, 593-597.
6. Lin, H.; Cornish, V. W. *Angew Chem Int Ed Engl* **2002**, *41*, 4402-4425.
7. Terstappen, G. C.; Schlupen, C.; Raggiaschi, R.; Gaviraghi, G. *Nat Rev Drug Discov* **2007**, *6*, 891-903.
8. Nguyen, T. N.; Goodrich, J. A. *Nat Methods* **2006**, *3*, 135-139.
9. Chen, G. I.; Gingras, A. C. *Methods* **2007**, *42*, 298-305.
10. Kim, Y. K.; Lee, J. S.; Bi, X.; Ha, H. H.; Ng, S. H.; Ahn, Y. H.; Lee, J. J.; Wagner, B. K.; Clemons, P. A.; Chang, Y. T. *Angew Chem Int Ed Engl* **2011**, *50*, 2761-2815.

11. Luo, Y.; Batalao, A.; Zhou, H.; Zhu, L. *Biotechniques* **1997**, *22*, 350-352.
12. Deane, C. M.; Salwinski, L.; Xenarios, I.; Eisenberg, D. *Mol Cell Proteomics* **2002**, *1*, 349-356.
13. Inglese, J.; Johnson, R. L.; Simeonov, A.; Xia, M.; Zheng, W.; Austin, C. P.; Auld, D. S. *Nat Chem Biol* **2007**, *3*, 466-479.
14. Kerppola, T. K. *Nat Protoc* **2006**, *1*, 1278-1286.
15. Kerppola, T. K. *Annu Rev Biophys* **2008**, *37*, 465-487.
16. Fernandez-Suarez, M.; Chen, T. S.; Ting, A. Y. *J Am Chem Soc* **2008**, *130*, 9251-9253.
17. Michnick, S. W. *Curr Opin Biotechnol* **2003**, *14*, 610-617.
18. Nguyen, A. W.; Daugherty, P. S. *Nat Biotechnol* **2005**, *23*, 355-360.
19. Komatsu, N.; Aoki, K.; Yamada, M.; Yukinaga, H.; Fujita, Y.; Kamioka, Y.; Matsuda, M. *Mol Biol Cell* **2011**, *22*, 4647-4656.
20. Zhang, J.; Campbell, R. E.; Ting, A. Y.; Tsien, R. Y. *Nat Rev Mol Cell Biol* **2002**, *3*, 906-918.
21. Giepmans, B. N.; Adams, S. R.; Ellisman, M. H.; Tsien, R. Y. *Science* **2006**, *312*, 217-224.
22. Heydorn, A.; Lundholt, B. K.; Praestegaard, M.; Pagliaro, L. *Methods Enzymol* **2006**, *414*, 513-530.
23. Lee, K. H.; Lee, S.; Lee, W. Y.; Yang, H. W.; Heo, W. D. *Proc Natl Acad Sci U S A* **2010**, *107*, 3412-3417.